Analysis of the fault geometry of a Cenozoic salt-related fault close to the D-1 well, Danish North Sea

Ole Rønø Clausen, Kenneth Petersen and John A. Korstgård

Abstract

A normal detaching fault in the Norwegian-Danish Basin around the D-1 well (the D-1 fault) has been mapped using seismic sections. The fault has been analysed in detail by constructing backstripped-decompacted sections across the fault, contoured displacement diagrams along the fault, and vertical displacement maps. The result shows that the listric D-1 fault follows the displacement patterns for blind normal faults. Deviations from the ideal displacement pattern is suggested to be caused by salt-movements, which is the main driving mechanism for the faulting. Zechstein salt moves primarily from the hangingwall to the footwall and is superposed by later minor lateral flow beneath the footwall. Backstripping of depth-converted and decompacted sections results in an estimation of the salt-surface and the shape of the fault through time. This procedure then enables a simple modelling of the hangingwall deformation using a Chevron model with hangingwall collapse along dipping surfaces. The modelling indicates that the fault follows the salt surface until the Middle Miocene after which the offset on the fault also may be accommodated along the Top Chalk surface.

Introduction

Structural hydrocarbon traps in a broad sense represent the habitat of the bulk of the already discovered petroleum reserves in the world. The cause for generation of the structural trap may vary from halokinesis, major faulting of the crust due to change in the regional horizontal stresses, differential compaction across former active faults and gravitationally introduced local changes in horizontal stresses. The latter involves not the faulting of the entire crust but only down to a dipping detachment surface of low viscosity material (most often undercompacted clays, or salt). The shape of the faults may vary from planar to listric the latter generating a roll-over anticline in the hangingwall sediments reflecting the shape of the fault plane (Crans and Mandl, 1980, Hamblin, 1965, Waltham, 1989, White et al., 1986). However, deformation of the volume of rock containing a fault (even a planar fault) will introduce a reverse drag on both the footwall and hangingwall of the fault (Barnett et al., 1987, Walsh and Watterson, 1987, Watterson, 1986) and the reverse drag may resemble the roll-over anticline. It is with respect to hydrocarbon prospectivity in the hangingwall roll-over anticlines of major importance to evaluate the generation of the anticline in time and space and compare it to the generation and migration of hydrocarbons. The fault investigated here is located in the Norwegian-Danish Basin (Fig. 1) is penetrated by the D-1 well, and will be called the D-1 fault hereafter. A number of different methods have been used to unravel the geological history of the D-1 fault. The methods and the results will be briefly described here with a focus on modelling of the hangingwall deformation through time.

Geological setting

The D-1 fault has a horizontal length of approximately 70 km, strikes ENE-WSW and down throws the Triassic to Late Tertiary sediments down to the NNW along a listric fault surface. The D-1 well (Fig. 2) has penetrated of Rotligendes volcanics, Zechstein evaporites (hereafter called Zechstein salt), Triassic, Jurassic, Cretaceous and Tertiary sediments. The Chalk Group (including the Late Cretaceous and Danian) constitutes a fairly thick layer compared to the Jurassic and Lower Cretaceous. However, it is striking that almost half of the total sedimentary succession consists of Tertiary sediments of Late Paleocene to Late

Miocene age. The pre-Oligocene Tertiary sediments are clay dominated whereas the Oligocene and younger sediments are dominated by cyclic input of clastic sediments of varying clay-sand ratio (Kristoffersen and Bang 1982). The Zechstein salt has periodically been mobile since Middle Triassic (Glennie, 1990, Ziegler, 1990).

Data

The mapping of the fault is based on the seismic surveys RTD-81, SP-82, DCS-81 and CGT-81 which cover the area in a dense grid and thus give control on the tie of horizons across the D-1 fault. The lithostratigraphic subdivision and dating for the pre-Tertiary sediments has been adopted from Nielsen and Japsen (1991) whereas the dating of the Tertiary horizons is taken from wells in the adjacent Central Trough area dated by Stouge (1988) and correlated to seismic section by Clausen (1991).

Fault analysis

The following horizons have been mapped and used in the fault analysis : Top pre-Zechstein (TPZ), Top Zechstein (TZ), Top Triassic (TTR), Base Upper Cretaceous (BUC), Top Chalk (TC), Intra Lower Miocene I (C1) Intra Lower Miocene 2 (C2) and Base Middle Miocene (C3). Fig. 3 shows the seismic appearance of the fault and the mapped horizons.

Displacement analysis

Displacement on a fault can be examined by analyzing the variations of throw along the fault plane and/or by analyzing the deformation introduced by a fault onto a given horizon.

The throw on a fault at given points tends to vary systematically with respect to the maximum throw at the fault center, fault width and distance from the fault center (Barnett et al., 1987, Walsh and Watterson, 1987, Watterson, 1986). One way to show the variations is a contoured displacement diagram where the throw values obtained from the seismic sections are projected onto a vertical plane parallel with fault strike (Fig. 4). The projected throw values are contoured and the contour pattern is a unique description of the throw variations along the fault plane. The ideal theoretical contour pattern is a full ellipse where the zero contour shows the location of the tip-line of the fault and the center of the contours shows the location of the fault center. Since the D-1 fault is a detaching listric fault the contours will be open downwards which however does not indicate that the fault continues downwards. The diagrams at C2-time, C3-time and present-day are shown in Fig. 5 and analyzed in detail in Petersen et al. (1992, 1993).

The depth maps (in TWT) of the Top Chalk Group and C2 (Fig. 6) show that the D-1 fault introduces systematic deviations from the regional trend of the horizons. The regional surface topography is interpreted across the deformed zone for each horizon and vertical displacement maps are constructed by subtracting the interpreted regional map from the depth map. The vertical displacement map thus shows the deformation of the hangingwall and the footwall introduced by the faulting without the disturbing effects of a palaeotopography or later differential basement subsidence (Fig. 7).

The displacement analysis shows that there are deviations from ideal displacements along the D-1 fault. This observation is interpreted to be a consequence of complex salt flow beneath the fault. The Zechstein salt, which became concentrated in a salt pillow during the Triassic, was reactivated during the Late Cretaceous (Petersen et al. 1992). The reconstructed salt-surface on the backstripped and decompacted sections (Fig. 8) indicate a flow of salt from the NNW to the SSE during the Late Cretaceous and the Tertiary controlling the displacement along the D-1 fault. The relative topographic low at the footwall of the

D-1 fault (east of the fault center) and the distorted contours on the contoured displacement diagrams indicates subsequent movements of salt from the ENE to the WSW beneath the footwall. The salt movements caused the very steep closure on the footwall at the center of the D-1 fault as indicated on both the depth maps and the vertical displacement maps.

Shape of the fault-plane

The shape of the fault plane is controlling the hangingwall geometry (Waltham, 1989, White et al., 1986). The variations of the fault plane geometry in time and space is examined by depth-converting, decompacting and backstripping the sections oriented at approximately 90° to the strike of the D-1 fault (Fig 8). During the backstripping the fault beneath the Zechstein salt has been regarded as inactive, and the regional topography of the basement is used as reference level (details in the backstripping and decompaction procedure are given in Petersen et al. (1993)). This procedure enables the construction of the salt surface and the fault geometry through time (Petersen et al. 1993). The salt movements inferred from this approach confirm the interpretations from the displacement analysis. The analysis also shows that the fault shape is both a consequence of compaction across the fault and of the location of the salt structure since the salt is regarded as non-compacting. In addition to the deformation of the horizons the upward movements of the salt have also affected the fault plane geometry.

The fault shape at different times obtained from the backstripping and decompaction have been used in a simple forward modelling of the hangingwall deformation. The modelling of the hangingwall deformation on a horizon uses a simple Chevron model with hangingwall collapse along inclined shear surfaces.

To minimize the influence of the salt movements beneath the hangingwall the effect of a given fault plane geometry is only examined onto the latest deposited horizon. This procedure implies that the geometry of the Top Chalk horizon is modelled using the geometry of the fault plane at C1 time, the geometry of the C1 horizon is modelled using the geometry of the fault plane at C2 time, etc. (Fig. 9).

The modelled geometries of the pre-C3 horizons approximate those obtained by backstripping the seismic sections when assuming a fault plane that detaches approximately along the top of the Zechstein salt structure (Fig. 9). However, using a fault detaching along the northern flank of the salt structure does not provide a geometry of the C3-horizon similar to the one obtained during the backstripping. A satisfactorily predicted geometry of the C3-horizon may instead be obtained by selecting a fault detachment along the present Top Chalk surface. The extension across the D-1 fault may thus be accommodated along two detachments, since it is impossible to exclude slip along the top of the Zechstein. The Late Paleocene and Eocene siliciclastic sediments deposited on the Top Chalk surface are dominated by clays, which in large areas are undercompacted. The shear strength of the clay may thus be reduced significantly. Furthermore, the dip of the Top Chalk surface is also to the NNW indicating that a generally northward movement along the Top Chalk surface is possible. The internal structures of the Late Paleocene-Eocene sediments in the hangingwall also show thinning close to the fault and thickening away from the fault associated with internal deformation of the sediments supporting a detachment along the Top Chalk surface (Petersen et al. 1993).

Conclusions

The geometrical analysis of the D-1 fault shows that
i. Although the fault differs fundamentally from the ideal blind normal fault of Watterson (1986) many of the geometrical relationships are similar giving good constraints on the lateral tie of detaching faults.

ii. Reactivation of a Zechstein salt pillow generated in the Triassic controlled the evolution of the D-1 fault geometry.

iii. Salt below the fault moved primarily from the hangingwall area into the footwall area, and secondarily laterally below the footwall generating a steep northern slope along which the D-1 fault detached during the period when the main offset took place.

iv. A combination of compaction and salt-induced deformation of the overburden changes the shape of the fault plane making the hangingwall deformation through time complex and enabling the possible generation of an additional detachment along the Top Chalk surface. However, the introduction of this bipartition of detachment is controversial and a better modelling of the bed geometries, determination of the possible overpressure in the undercompacted clays above the Top Chalk and analysis of possible stress configurations are necessary.

References

Barnett, J. A. M., Mortimer, J., Rippon, J. H., Walsh, J. J. and Watterson, J. 1987. Displacement geometry in the volume containing a single normal fault. American Association of Petroleum Geologists Bulletin, 71, 925-937.

Clausen, O. R. 1991. Tertiary seismic stratigraphic and structural evolution of the northern Danish Central Trough. PhD thesis, Aarhus University, 320 pp.

Crans, W. and Mandl, G. 1980. On the theory of growth faulting part II(a): Genesis of the unit. Journal of Petroleum Geology, 3, 209-236.

Glennie, K. W. 1990. Introduction to the Petroleum Geology of the North Sea. 3rd edition. Blackwell, London. 402 pp.

Hamblin, W. K. 1965. Origin of "reverse drag" on the downthrown side of normal faults. Geological Society of America Bulletin, 76, 1145-1164.

Kristoffersen, F. N. and Bang, I. 1982. Cenozioc excl. Danian limestone. In: Michelsen, O. (ed.) Geology of the Danish Central Graben. Danmarks Geologiske Undersøgelse, Series B, no. 8, 61-70.

Nielsen, L. H. and Japsen, P. 1991. Deep wells in Denmark 1935-1990. Danmarks Geologiske Undersøgelse, Serie A, Nr. 31, 177 pp.

Petersen, K., Clausen, O. R. and Korstgård, J. A. 1992. Evolution of a salt-related listric growth fault near the D-1 well, block 5605, Danish North Sea: displacement history and salt kinematics. Journal of Structural Geology, 14, 565-577.

Petersen, K., Clausen, O. R. and Korstgård, J. A. 1993. Evolution of a Salt-Related Tertiary Growth Fault in the Danish North Sea. In A.M Spencer (ed): Generation, Accumulation and Production of Europe's Hydrocarbons III. Special Publication of the European Association of Petroleum Geoscientists No 3, 69-78.

Stouge, S. 1988. Biostratigraphy of selected wells from the northwestern part of the Danish Central Trough. Internal CENBAS report, 63 pp.

Sørensen, K. 1986. Danish Basin subsidence by Triassic rifting on a lithosphere cooling background. Nature 319, 660-663.

Walsh, J. J. and Watterson, J. 1987. Distributions of cumulative displacement and seismic slip on a single normal fault surface. Journal of Structural Geology, 9, 1039-1046.

Waltham, D. 1989. Finite difference modelling of hangingwall deformation. Journal of Structural Geology, 11, 433-437.

Watterson, J. 1986. Fault dimensions, displacements and growth. Pure and Applied Geophysics, 124, 365-373.

White, N. J., Jackson, J. A. and McKenzie, D. P. 1986. The relationship between the geometry of normal faults and that of the sedimentary layer in their hanging walls. Journal of Structural Geology, 8, 897-909.

Ziegler, P. A. 1990. Geological Atlas of Western and Central Europe. Elsevier, Amsterdam. 239 pp.

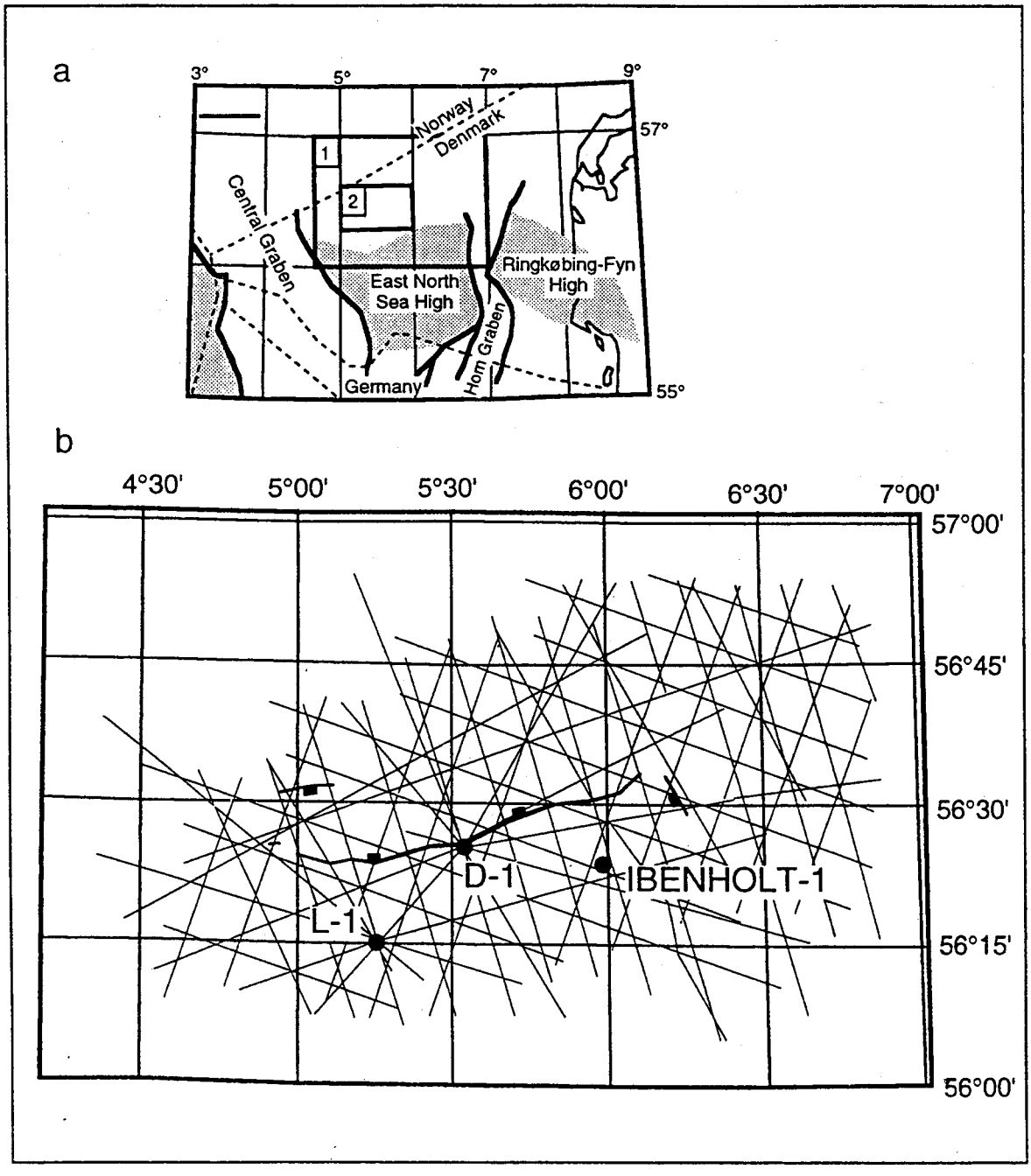

Fig. 1
a.The location of the studied area is indicated by box no. 1 which outlines the map border of Figs. 1b, 6a and 6b. Box no. 2 outlines the map border of Figs. 7a and 7b.
b. Map showing the D-1 fault cutting the Top Chalk level and the traces of the seismic lines used in the study.

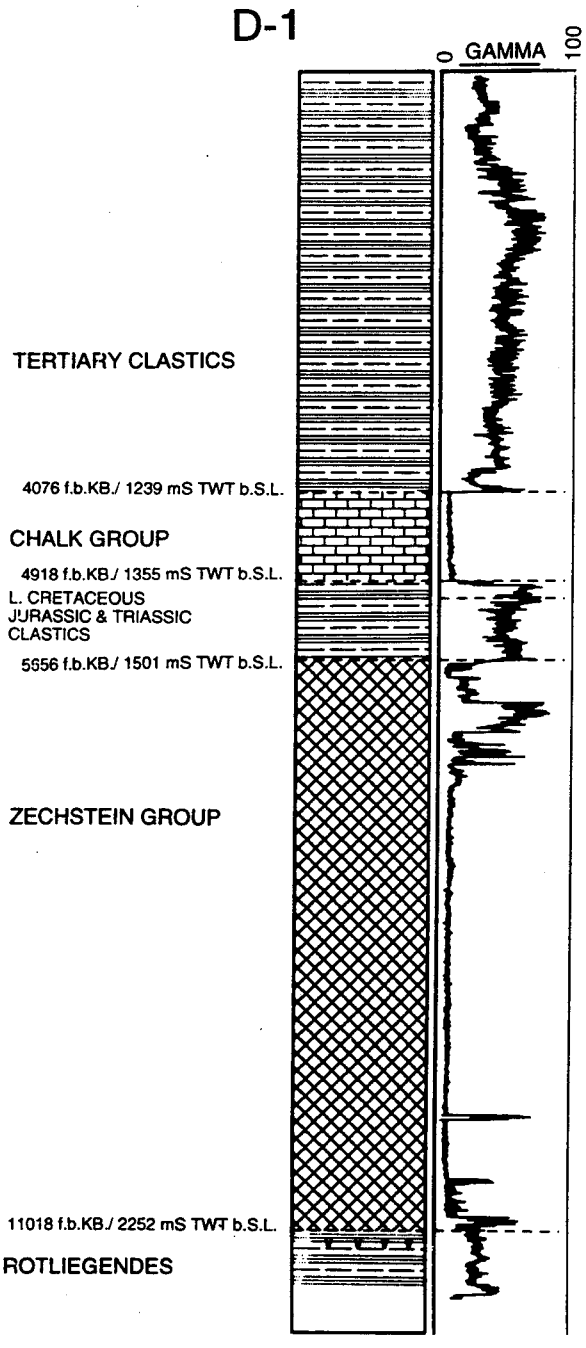

Fig. 2 Lithology and stratigraphy of the D-1 well (after Nielsen and Japsen, 1991) and associated gamma ray log curve.

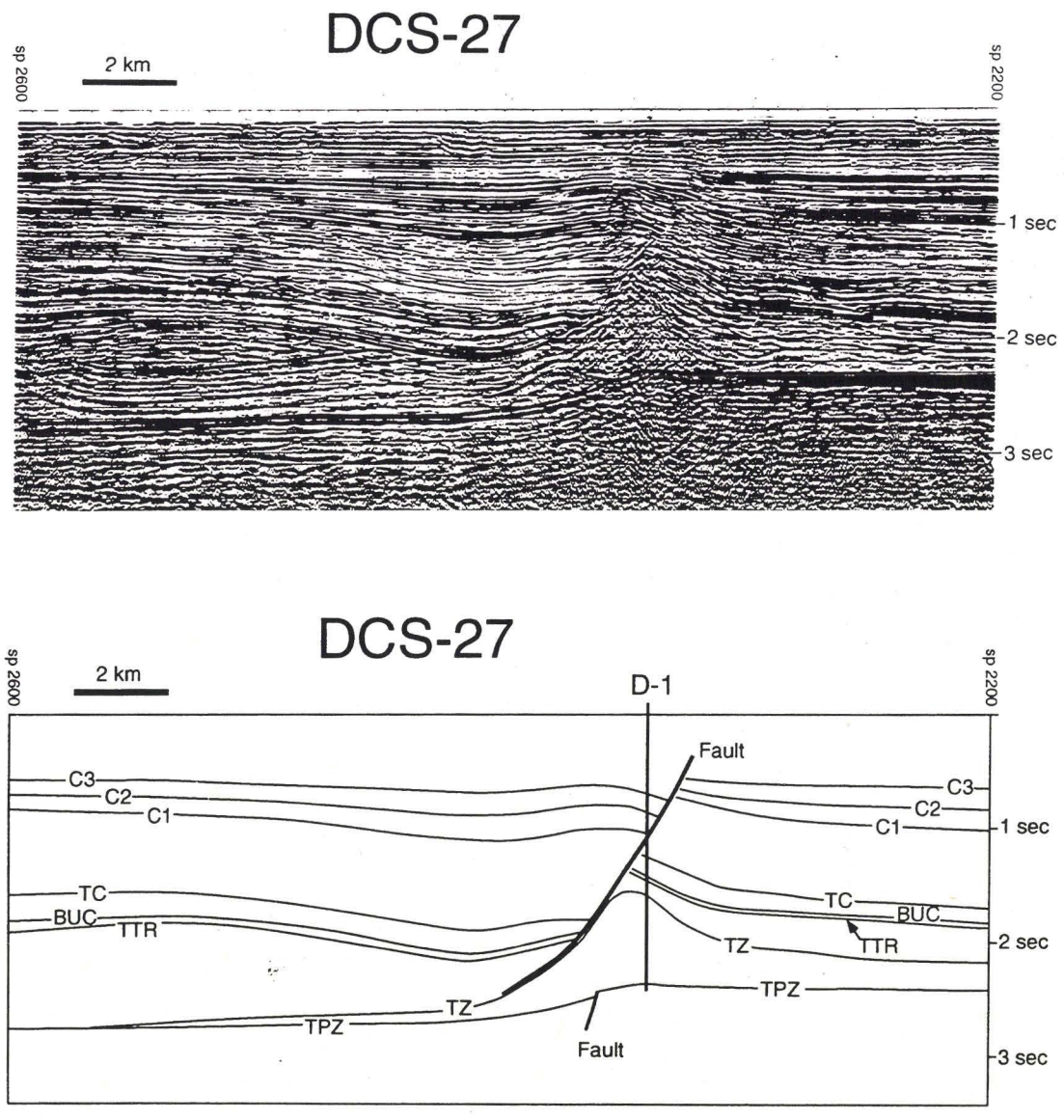

Fig. 3 Seismic line and line-drawing of DCS-27 which is cut by the D-1 well. The interpreted horizons are indicated and their ages are as follows: TPZ - Top Pre-Zechstein; TZ - Top Zechstein; TTR - Top Trias; BUC - Base Upper Cretaceous; TC - Top Chalk (top Cretaceous-top Danian); C1 - Intra Early Miocene; C2 - Intra Early Miocene and C3 - Base Middle Miocene.

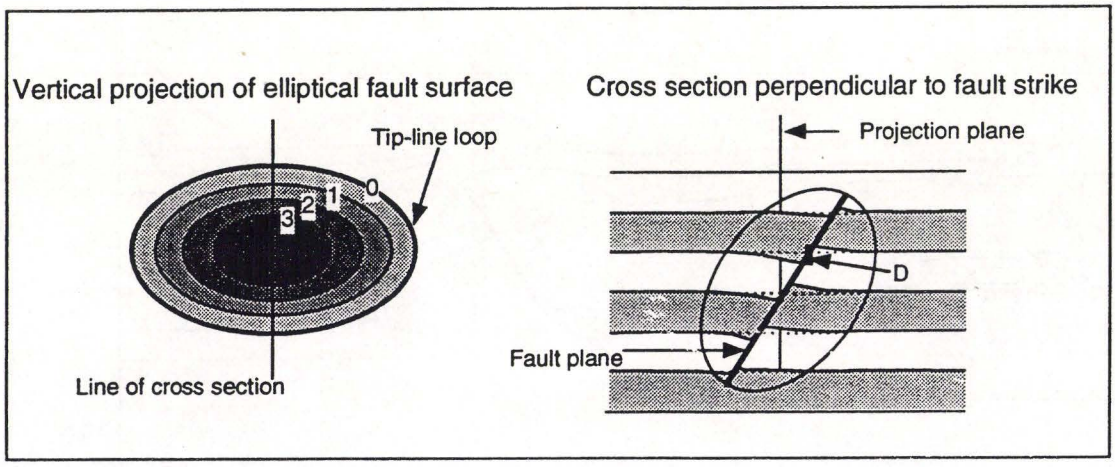

Fig. 4 Principles in determining the throw values and projecting them onto a vertical section parallel with the fault strike. The values are contoured and the result is a contoured displacement diagram, which uniquely describes the displacement on the fault (Barnett et al., 1987).

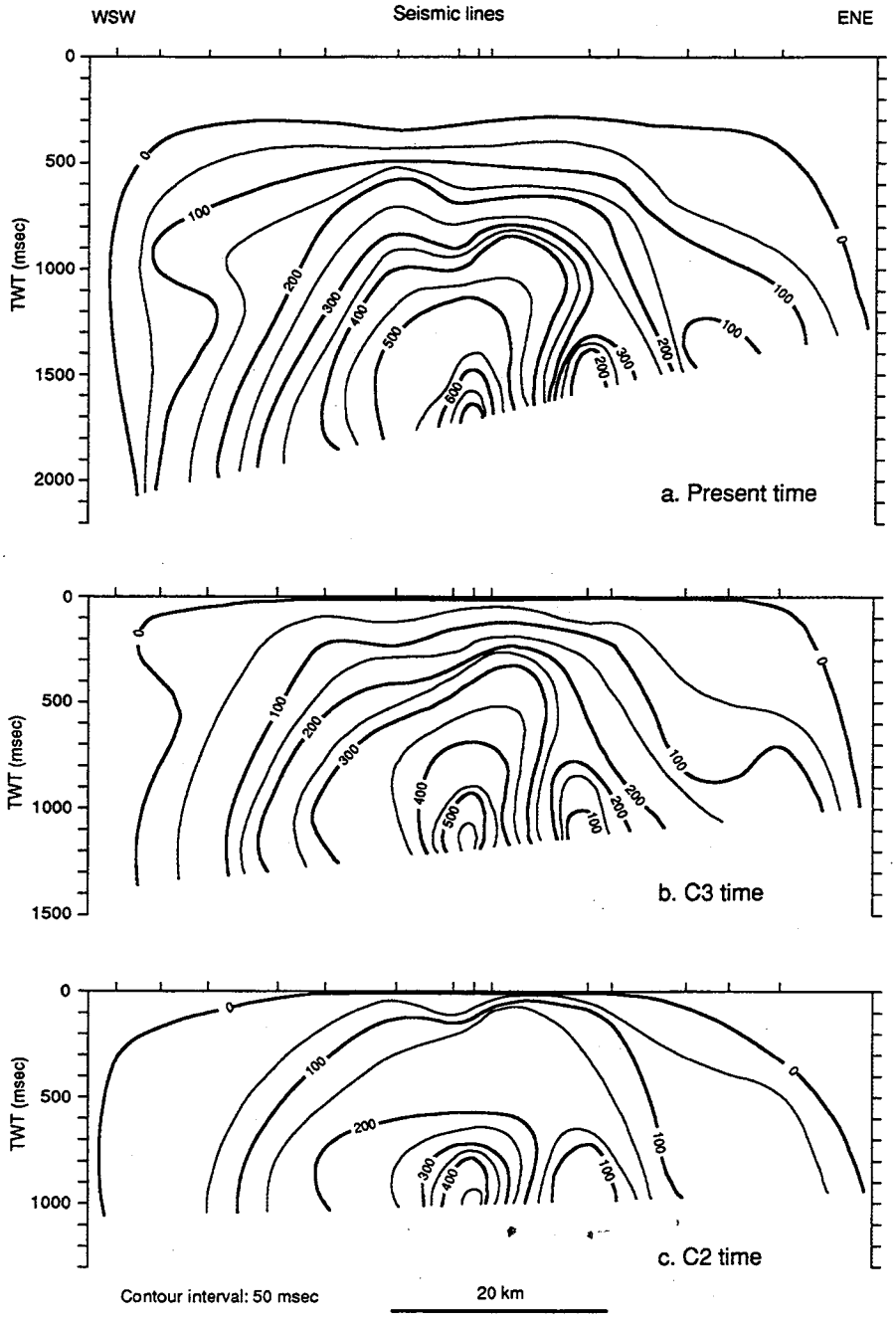

Fig. 5 Contoured displacement diagrams from the D-1 fault at present (a) and backstripped to C3 time (b) and C2 time (c). Displacement values are from 5 mapped horizons.

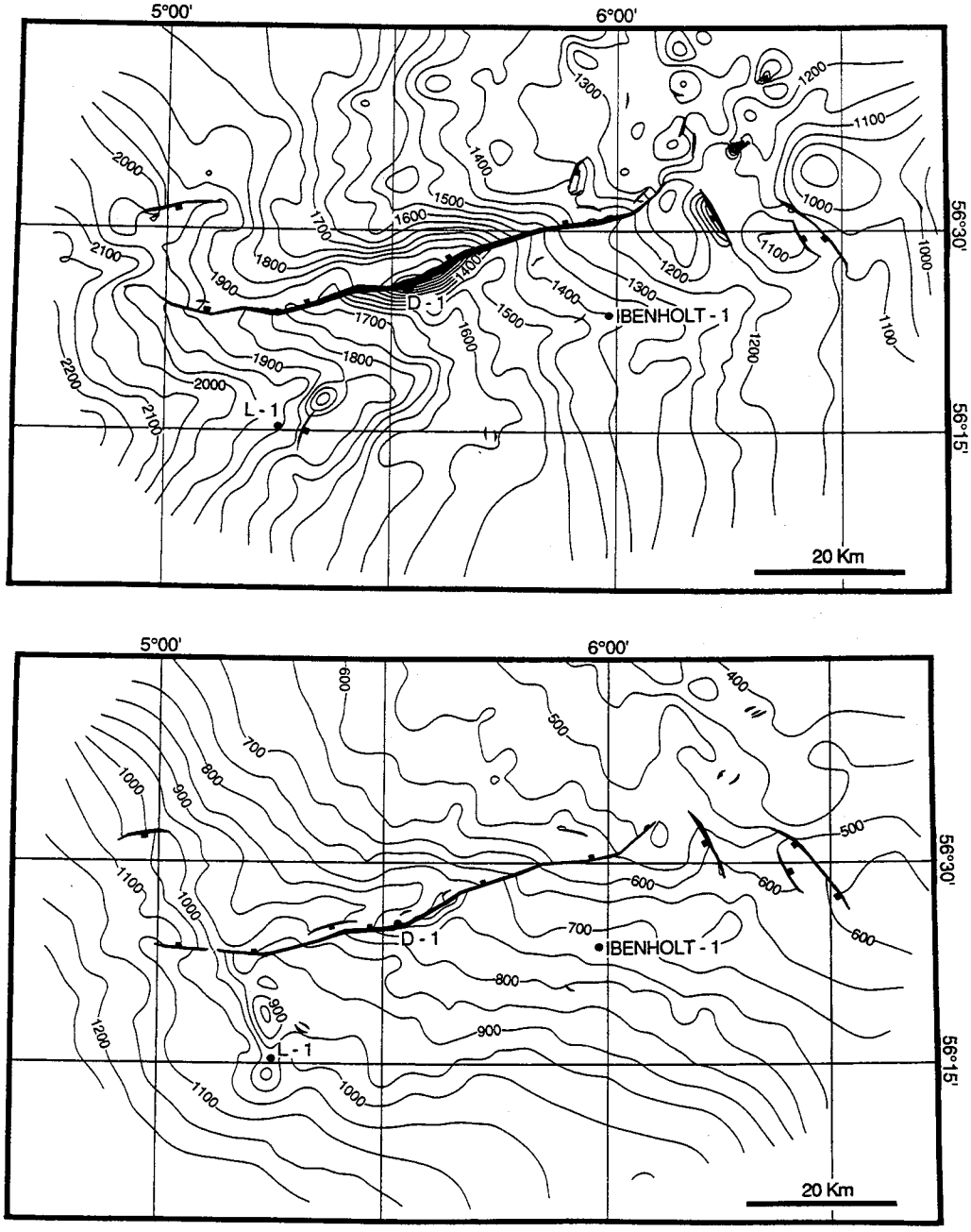

Fig. 6 Depth maps (TWT) of the Top Chalk (a) and C2 horizons (b). The regional dip on the horizons is distorted by the D-1 fault. The distortions are more prominent at the Top Chalk surface which emphasizes that the Top Chalk has suffered more deformation than the younger horizons.

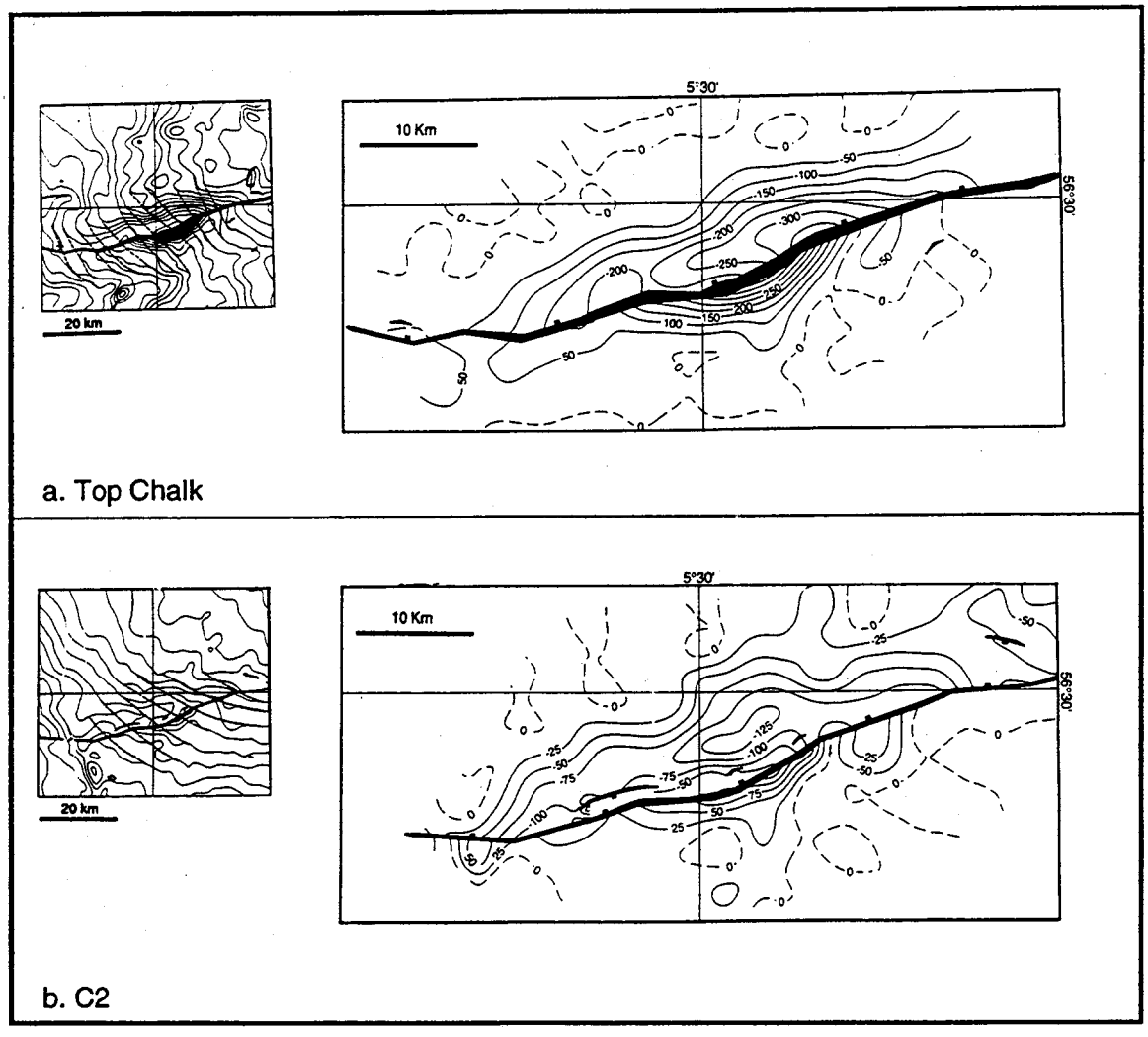

Fig. 7 Vertical displacement maps of the Top Chalk (a) and C2 (b) horizons. The inserted map shows the topography of the horizon with the interpreted regional (dashed lines). The footwall shows positive uplift except to the east, where a minor area shows subsidence with respect to the interpreted regional. The hangingwall shows subsidence but not symmetrically with respect to the footwall uplift.

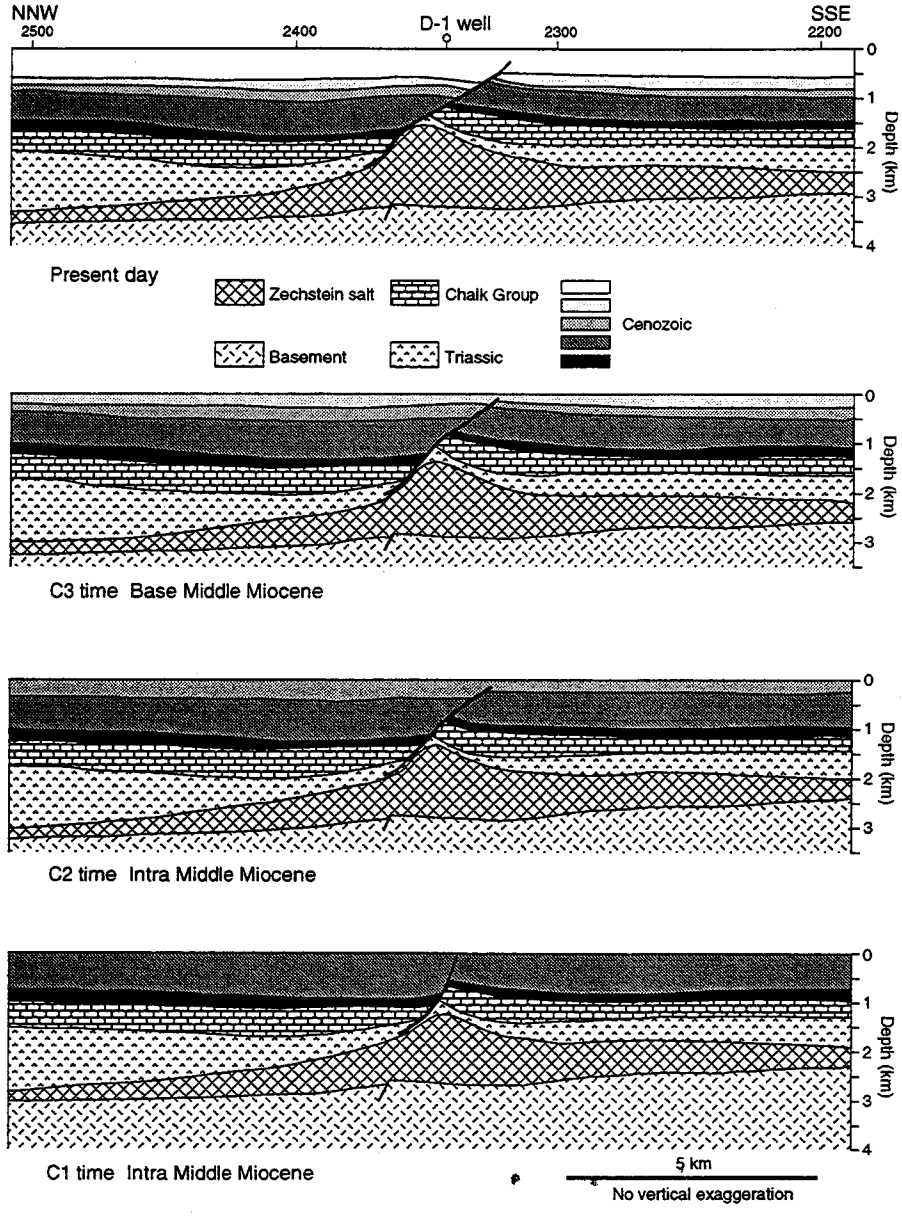

Fig. 8 Seismic section DCS-27 depth is converted and backstripped. The stratigraphicn sections are decompacted using the surface porosity and compaction parameters of Sørensen (1986). The change in shape of the D-1 fault and the salt structure is evident.

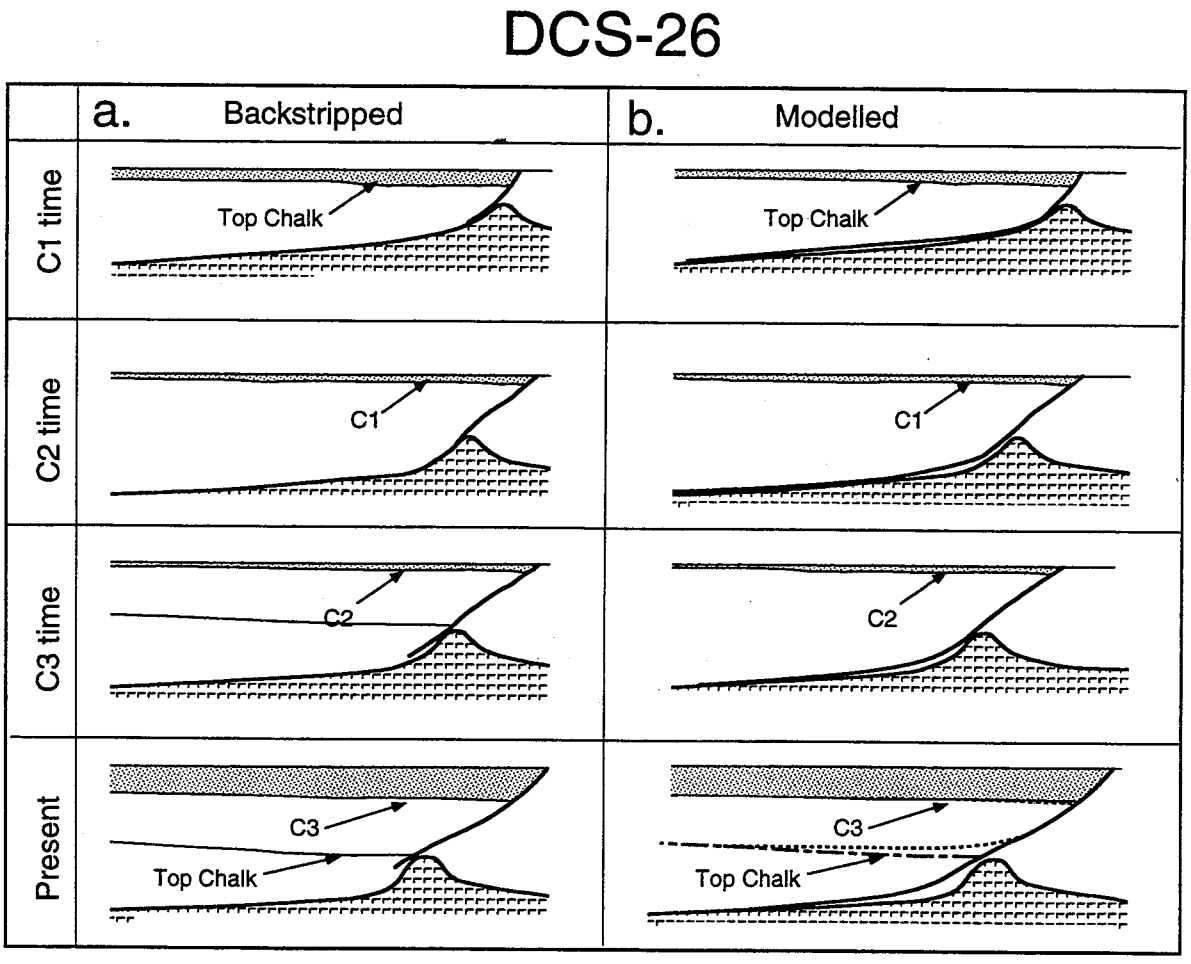

Fig. 9 The topography of the latest deposited but yet deformed horizon and the D-1 fault through time is shown in (a). The topography is derived from the backstripped section. In (b) is shown the corresponding modelled topography assuming a fault plane as shown. It is evident that the topography of the hangingwall horizons may be reproduced by a fault detaching along the Top Zechstein salt. However, the C3 horizon modelled does not fit the observed. The dashed line shows the closest fit using the dashed fault, whereas the full line shows the geometry achieved by using a fault detaching along the Top Zechstein salt surface. For further see text.